



HOKKAIDO UNIVERSITY

Title	Morphological and cytochemical studies of fertilization of <i>Palmaria</i> sp. (Rhodophyta)
Author(s)	Mine, Ichiro
Citation	北海道大學理學部海藻研究所歐文報告, 9(2), 111-139
Issue Date	1997-02
Doc URL	https://hdl.handle.net/2115/48113
Type	departmental bulletin paper
File Information	9(2)_111-139.pdf



Morphological and cytochemical studies of fertilization of *Palmaria* sp. (Rhodophyta)* **

By

ICHIRO MINE***

Introduction

Fertilization in red algae is achieved by fusion between a non-flagellated spermatium liberated from a male gametophyte, and a trichogyne, the specialized process of a carpogonium (egg cell) formed on a female gametophyte. The occurrence of amoeboid movement in red algal spermatia has frequently been noted (DIXON 1973) and extension of the trichogyne toward spermatia attached to the thallus surface (HOMMERSAND and FREDERICQ 1990) has been reported. Therefore, it is difficult to exclude chemotactic and chemotropic processes in gamete recognition in red algae. However, it is probable that taxon- and organ-specific recognition and attachment between red algal gametes are principally managed by the adhesiveness of the cell surface structures of the gametes (DIXON 1973, KIM and FRITZ 1993a). Red algal gametes provide good materials for studying specific cell-to-cell adhesion.

Several other physiological events are also indispensable for fertilization processes in red algae. Following successful attachment of a spermatium, localized cell wall breakdown of a trichogyne must occur before cytoplasmic fusion of the gametes. The male nucleus that invades from the fused spermatial cell must migrate scores of micrometers inside the trichogyne toward the base of the carpogonium where it can fuse with the carpogonial nucleus. It has also been reported that spermatial nuclear divisions are ordinarily completed at a certain stage of fertilization (FRITSCH 1945, p. 597 for references; GOFF and COLEMAN 1984).

Thus, fertilization in red algae includes many interesting processes for cell biologists, each of which will require detailed ultrastructural studies (PUESCHEL 1990, p. 31). There have been a number of reports on the ultrastructure of spermatogenesis and released spermatia as well as on the development of the diploid carposporophyte after fertilization

*Based on a dissertation in partial fulfillment of the requirements for the degree of Doctor of Science, Institute of Algological Research, Faculty of Science, Hokkaido University in 1993.

**Dedicated to Professors MASAKAZU TATEWAKI and TADAO YOSHIDA on the occasion of their academic retirement.

***Present address: Department of Biology, Faculty of Science, Kochi University, Akebono-cho 2-5-1, Kochi 780 Japan.

(PUESCHEL 1990, pp. 31, 32 for references). However, the majority of studies on the attachment and fusion between spermatia and trichogynes are restricted to light microscopic observations.

It has been shown using the scanning electron microscope (SEM) that spermatial appendages are specifically bound to the surfaces of the female gametes in *Aglaothamnion* (MAGRUDER 1984), *Bangia* (COLE *et al.* 1985) and *Antithamnion* (KIM and FRITZ 1993a). There have been a few ultrastructural studies on these events using the transmission electron microscope (TEM), e.g., observations on field-collected *Porphyra* (HAWKES 1978) and TEM figures of trichogynes before and after fertilization in *Polysiphonia* (BROADWATER and SCOTT 1982). However, there appear to be no TEM studies on the time-course changes in attachment and fusion of red algal gametes.

The lack of such information may be due to the difficulties in obtaining sufficient numbers of mature carpogonia in the red algae except for the bangiacean and palmariacean algae. In the female gametophytes of the bangiacean algae, e.g., species of *Bangia* and *Porphyra*, almost all cells of the fertile portion on the thalli develop into carpogonia as judged by the formation of zygotosporangia (e.g., HAWKES 1978, COLE *et al.* 1985). This advantageous feature is one of the reasons that the ultrastructures of several stages during fertilization have been investigated only in *Porphyra gardneri* (HAWKES 1978). There remain, however, certain problems concerning synchrony in carpogonial maturation. It seems to be difficult to distinguish mature unfertilized carpogonia from immature or vegetative cells before spermatium inoculation. Therefore, experimental studies using a sufficient number of simultaneously-matured carpogonia may be difficult in the bangiacean algae.

On the other hand, the palmariacean algae show a distinctive life history in which haploid tetraspores grow into either macroscopic male gametophytes and dwarf female gametophytes (VAN DER MEER and TODD 1980, VAN DER MEER 1981). Fertilization in these algae has been observed between spermatia released from the male macrothallus, and a sessile carpogonium developed on the microscopic female thalli. Using these algae, it is possible to obtain a number of simultaneously-matured carpogonia on dwarf female germlings and, consequently, the palmariacean algae provide a good experimental system for studying fertilization processes in red algae.

Along the Japanese coast, the palmariacean life history has been described in *Palmaria* sp. (DESHMUKHE and TATEWAKI 1990; as *Palmaria palmata* O. KUNTZE) and *Halosaccion yendoi* I. K. LEE (MINE and TATEWAKI 1993). The former species was chosen for studies on fertilization, and several morphological and cytochemical features of gametes that concern gamete attachment and fusion of this alga have been demonstrated (MINE and TATEWAKI 1994a, b). In this article, I summarize these studies on fertilization in *Palmaria* sp. along with some unpublished results from recent investigations in order to provide fundamental information for further research on the mechanisms of fertilization in

red algae.

Acknowledgements

I am very grateful to Professor MASAKAZU TATEWAKI for his kind guidance and encouragement during the present study. I would like to express thanks to Dr. TAIZO MOTOMURA for his kind teaching of electron microscopic techniques and helpful suggestions. Special thanks go to Dr. TERUNOBU ICHIMURA for his critical reading of the manuscript and for improving the English usage. I also thank Drs. ISAMU WAKANA and GEETANGELI V. DESHMUKHE for giving friendly and practical advice. And I greatly appreciate the many types of assistance provided by the staff and graduate students of the Institute of Algological Research.

Materials and Methods

Preparation of male and female gametes, and spermatium inoculation

Mature thalli of *Palmaria* sp. were collected from January to June of 1991, 1992 and 1993 at Charatsunai, Muroran, Hokkaido, Japan. Preparation of spermatial suspensions and mature female germings, and spermatium inoculation were conducted as described previously (MINE and TATEWAKI 1994a). Samples were fixed for DNA fluorescence microscopy or TEM observations at the desired time after the onset of spermatium inoculation.

Sample preparation for fluorescence microscopy and TEM

Nuclear staining of samples with 4', 6-diamidino-2-phenylindole (DAPI) and detection of cell walls using calcofluor white M2R were done according to MINE and TATEWAKI (1994a). Observations were carried out with an Olympus BH2-RFK epifluorescence microscope using "U-excitation". Photographs were made with Fuji Neopan F for DAPI-stained samples and Kodak Tri-X for calcofluor staining.

For preparation of TEM specimens, Methods A (fixatives containing NaCl, *en bloc* staining in aqueous uranyl acetate and embedment in Spurr's resin), B (sucrose, uranyl acetate in 70% acetone and Spurr's resin) and C (fixatives containing ruthenium red and embedment in LR white resin) in MINE and TATEWAKI (1994a) were also used in the present study and indicated as Methods A, B and C, respectively. In addition, two other methods described below were adopted in the present study.

Method D. To observe the spermatial covering during spermatogenesis and enhance the trichogyne coat, samples were fixed in 0.1 M cacodylate buffer (pH 7.2) containing 3% glutaraldehyde and 2% NaCl for 2 h at 4°C, washed in buffer containing NaCl, rinsed with water, dehydrated in ethanol, and embedded in LR white resin.

Method E. Observations of membranous structures in the trichogyne cytoplasm were made on specimens which were postfixed with osmium fixative containing potassium fer-

ricyanide. Samples were fixed in 3% glutaraldehyde, 2% NaCl in 0.1 M cacodylate buffer for 60 min. After rinsing with buffer containing NaCl, the samples were then postfixed in osmium tetroxide with 0.8% potassium ferricyanide in buffer. The postfixed samples were washed in buffer containing NaCl, rinsed with water, dehydrated in acetone, and embedded in Spurr's resin.

Thin sections were cut using a diamond knife on a Porter-Blum MT-1 ultramicrotome, stained with lead citrate, and observed with a Hitachi H-300 transmission electron microscope. The sections of the samples prepared by Methods D and E were stained with both uranyl acetate (4% in water) and lead citrate.

Degradation of gamete surfaces and estimation of gamete attachment

Digestion of spermatial covering by proteases was carried out according to MINE and TATEWAKI (1994b). Vicinal glycol residues in the trichogyne coat were detected by the periodic acid-thiocarbohydrazide-silver proteinate (PATAg) test and degraded by oxidation with periodic acid followed by reduction with sodium borohydride as described previously (MINE and TATEWAKI 1994b).

After degradation of the surface component, gametes were subjected to comparative spermatium inoculation and the resulting gamete attachment was estimated quantitatively as described in MINE and TATEWAKI (1994b).

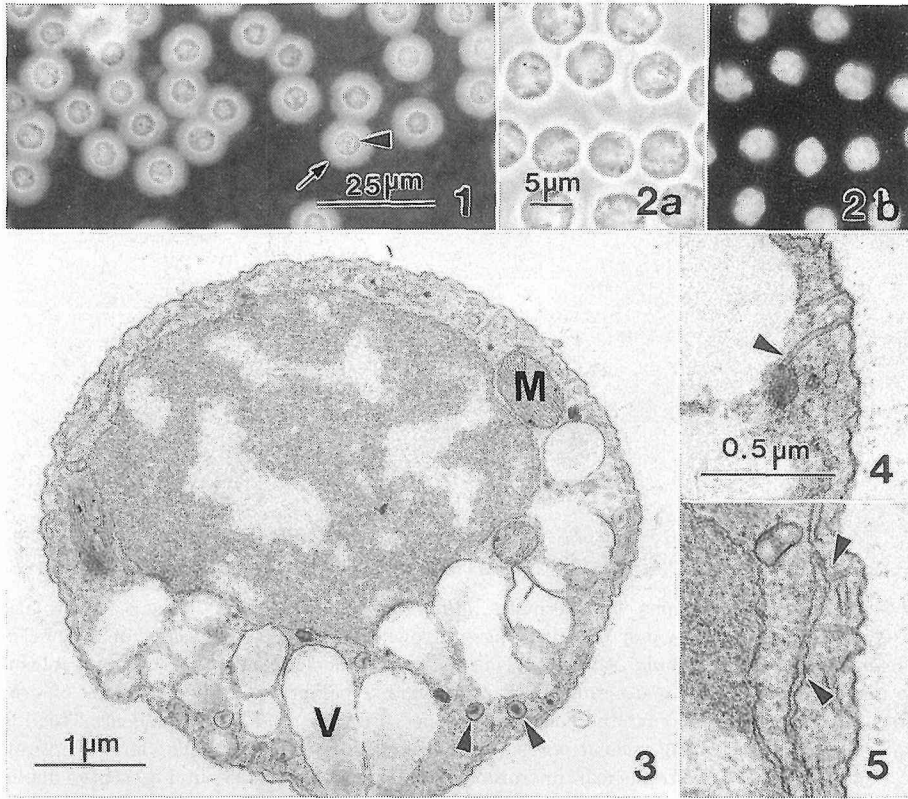
Results

Spermatia

Viewed under the light microscope, liberated spermatia were spherical, colorless, ca. 5 μm in diameter (Fig. 1) and composed of a cytoplasmic region and a relatively larger vacuolar region (Fig. 2a). The cytoplasmic region was principally occupied by a highly condensed nucleus (Fig. 2b). Autofluorescence of plastids was not detected under the fluorescence microscope.

Observations of TEM specimens also revealed that the vacuolar region consisted of large, electron-transparent vesicles, whereas the cytoplasm was largely occupied by a condensed nucleus (Fig. 3). Small, electron-dense vesicles, endoplasmic reticulum (ER), and tubular structures were present near the cell periphery (Figs. 3-5). The peripheral tubules were apparently continuous with the plasma membrane, and closely associated with electron-dense vesicles (Fig. 4) or peripheral ER (Fig. 5).

The condensed spermatial nucleus was in prophase, because it had established two opposite division poles, as indicated by the presence of a polar ring (PR), a nucleus-associated organelle in red algae (SCOTT and BROADWATER 1990) (Figs. 6-8). The PRs were surrounded by electron-dense material and located above a depression of the nuclear envelope (Figs. 6, 7). Microtubules (MTs) were also observed around PRs in both the extranuclear and intranuclear regions (Figs. 7, 8) and most of these MTs were radiated



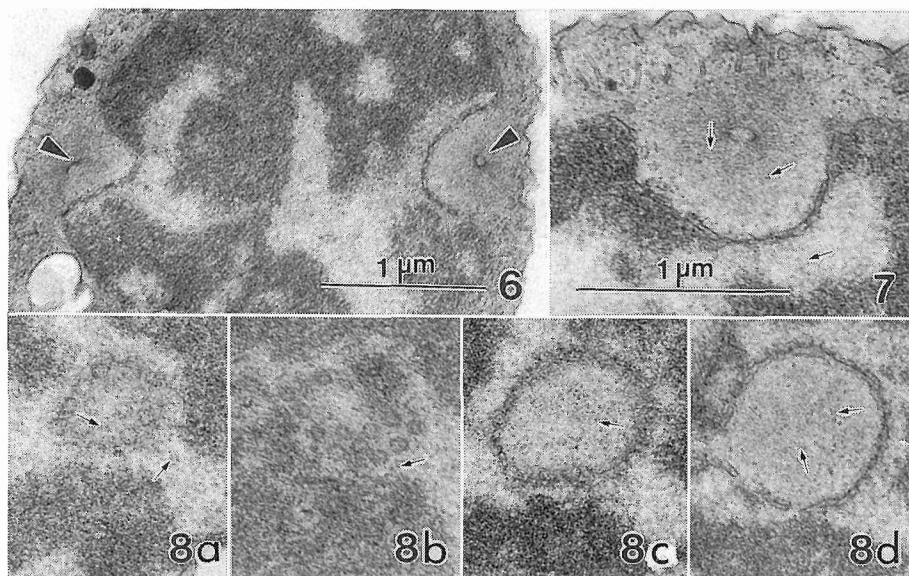
Figs. 1-5. Liberated spermata of *Palmaria* sp.

Figs. 1, 2. Light micrographs. Fig. 1. Co-aggregated cells. Non-fixed material. Prepared in India ink/seawater. The cells (arrowhead) are covered with colorless coverings (arrow). Fig. 2. DAPI-stained. a) Phase contrast and b) Epifluorescence. Figs. 3-5. TEM micrographs. Prepared by Method A. Fig. 3. Median section showing a condensed spermatial nucleus, large vesicles (V), mitochondria (M) and small, electron-dense vesicles (arrowheads). Figs. 4, 5. Cell periphery. Scale in Fig. 4 also applies to Fig. 5. Fig. 4. Close association of peripheral tubules with electron-dense vesicles (arrowhead). Fig. 5. Peripheral tubules associated with peripheral endoplasmic reticulum (arrowheads).

from PRs (Fig. 8). However, continuity between the extranuclear and intranuclear MTs was not discovered.

Spermatial covering

Liberated spermata had a colorless, ca. 3 μm -thick covering which was visible in the specimens prepared with India ink (Figs. 1, 11). The TEM specimen fixed by Method C showed a fibrous, reticulated configuration of the spermatial covering on the plasma mem-

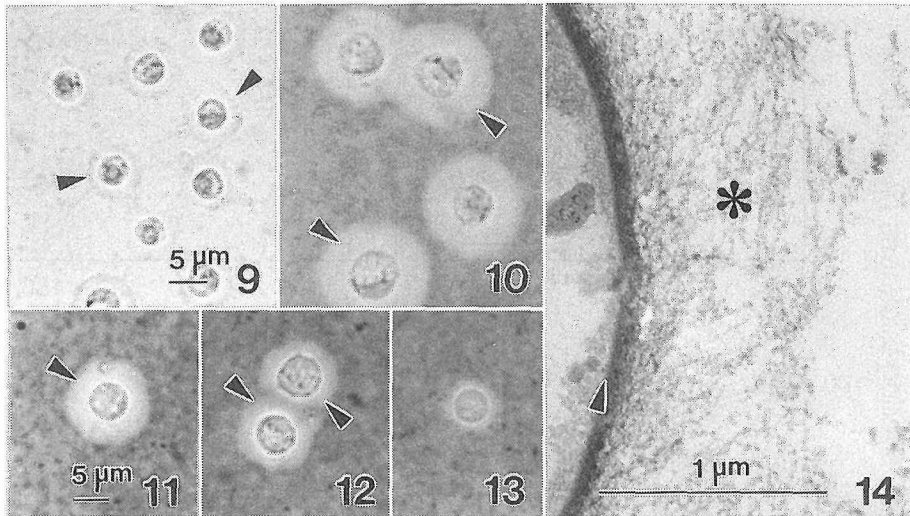


Figs. 6-8. TEM micrographs of spermatia. Prepared by Method A. Fig. 6. Spermatial nucleus accompanied with a pair of polar rings (arrowheads) above depressions of the nuclear envelope. Fig. 7. An example of a polar ring in another nucleus. Some extra- and intranuclear microtubules (arrows) are radiated from around a polar ring. Fig. 8. Series of cross sections of a polar depression of the nuclear envelope. Figs. 8a and 8b are tangential sections of nuclear envelopes showing nuclear pores. Arrows indicate cross or oblique views of intranuclear (Figs. 8a, 8b) and extranuclear microtubules (Figs. 8c, 8d). Scale in Fig. 7 also applies to Fig. 8.

brane of spermatia (Fig. 14).

The spermatial covering exhibited a semi-solid, or gel-like property. During gradual dehydration after glutaraldehyde fixation of the cell, the covering gradually became thinner (Fig. 9). After a gradual 're-hydration' in water, the thickness was recovered (Fig. 10).

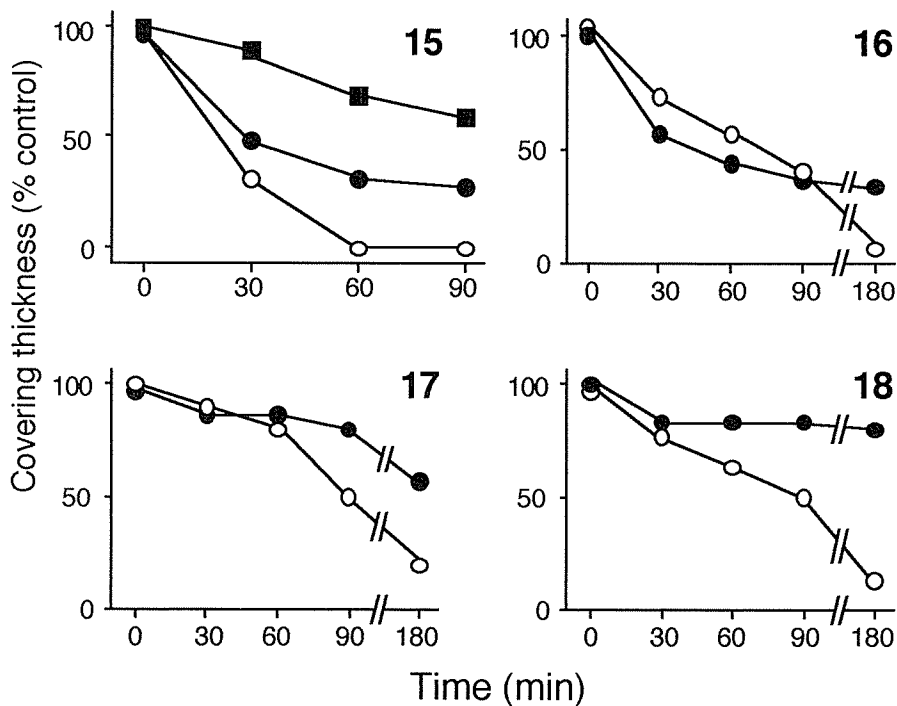
The thickness of the spermatial covering of the living spermatia decreased by protease treatment in both a concentration- and time-dependent manner (Figs. 11-13, 15, 16). The covering thickness decreased by protease treatment even in the glutaraldehyde-fixed spermatia (Fig. 17), and a protease inhibitor (phenylmethylsulfonyl fluoride) represented the decrease in the covering thickness by trypsin (Fig. 18). This appears to indicate that the decrease in the covering thickness is the result of enzymatic digestion of the protein(s) which constitute the covering rather than damage to the covering-generating activity of the living spermatium. In addition, gradual degradation of the spermatial covering by protease treatment was also observed in the TEM specimens (MINE and TATEWAKI 1994b).



Figs. 9-14. Spermatial coverings. Figs. 9-13. Light micrographs of spermatia. Prepared in India ink/seawater. Figs. 9, 10. Spermatia fixed in 1% glutaraldehyde in artificial seawater. Scale in Fig. 9 also applies to Fig. 10. Fig. 9. After gradual dehydration by 90% ethanol showing the outline of shrunken spermatial coverings (arrowheads) indicated by sediment of carbon particles of India ink. Fig. 10. After gradual 're-hydration' by water following dehydration. Thickness of the spermatial coverings (arrowheads) has recovered. Figs. 11-13. Non-fixed spermatia. Scale in Fig. 11 also applies to Figs. 12, 13. Fig. 11. Untreated cells. Colorless coverings (arrowhead) are uniformly observed around the cell. Fig. 12. Treated with 1% Pronase E for 30 min. The thickness of spermatial covering (arrowheads) has been decreased. Fig. 13. Treated with 1% Pronase E for 120 min. The spermatial covering cannot be detected. Fig. 14. TEM micrograph of median section of spermatium. Prepared by Method C. Plasma membrane (arrowhead) is covered with fibrous, reticulated spermatial covering (asterisk).

The spermatial coverings were uniformly observed on all liberated spermatia and the thickness appeared to be unchanged for at least several days after liberation. Therefore, it is probable that the covering was produced to completion during spermatial development before spermatium liberation. In the TEM specimens prepared by Method A, a number of electron-transparent vesicles were observed in the spermatangia. Some of these vesicles were secreted from the whole surface of the plasma membrane of the spermatial cell inside the spermatangial wall (Fig. 19), while the others remained within the cell to form the larger, electron-transparent vesicles in the vacuolar region of the liberated spermatium.

The secretion of vesicles was observed at an early stage of spermatangial development while the spermatangium was still connected with its parent cell by a pit connection (Fig. 19). In the specimens prepared by Method D, fibrous, reticulate structures apparently identical to the spermatial covering were observed both in the vesicles (Fig. 20) and in

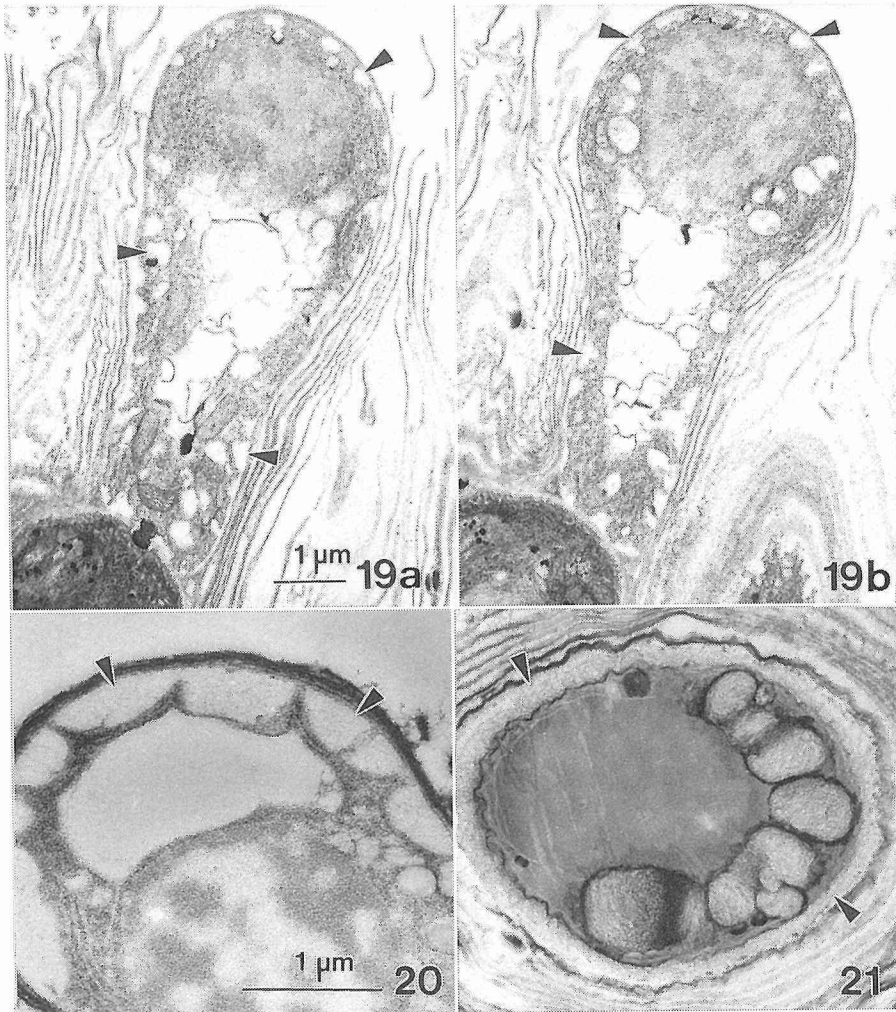


Figs. 15-18. Time courses of changes in thickness of spermatial coverings during treatment with proteases. The thickness of spermatial coverings is expressed as a percent of control. Data are redrawn from MINE and TATEWAKI 1994b. Figs. 15, 16. Non-fixed spermata. Fig. 15. Treated with 1% (white circle), 0.1% (black circle), or 0.01% (black square) Pronase E. Fig. 16. Treated with 1% trypsin (white circle), or 1% papain (black circle). Fig. 17. Glutaraldehyde-fixed spermata treated with 0.5% (white circle), or 0.1% (black circle) Pronase E. Fig. 18. Non-fixed spermata treated with 0.5% trypsin (white circle), or 0.5% trypsin along with 1 mM phenylmethylsulfonylfluoride (black circle).

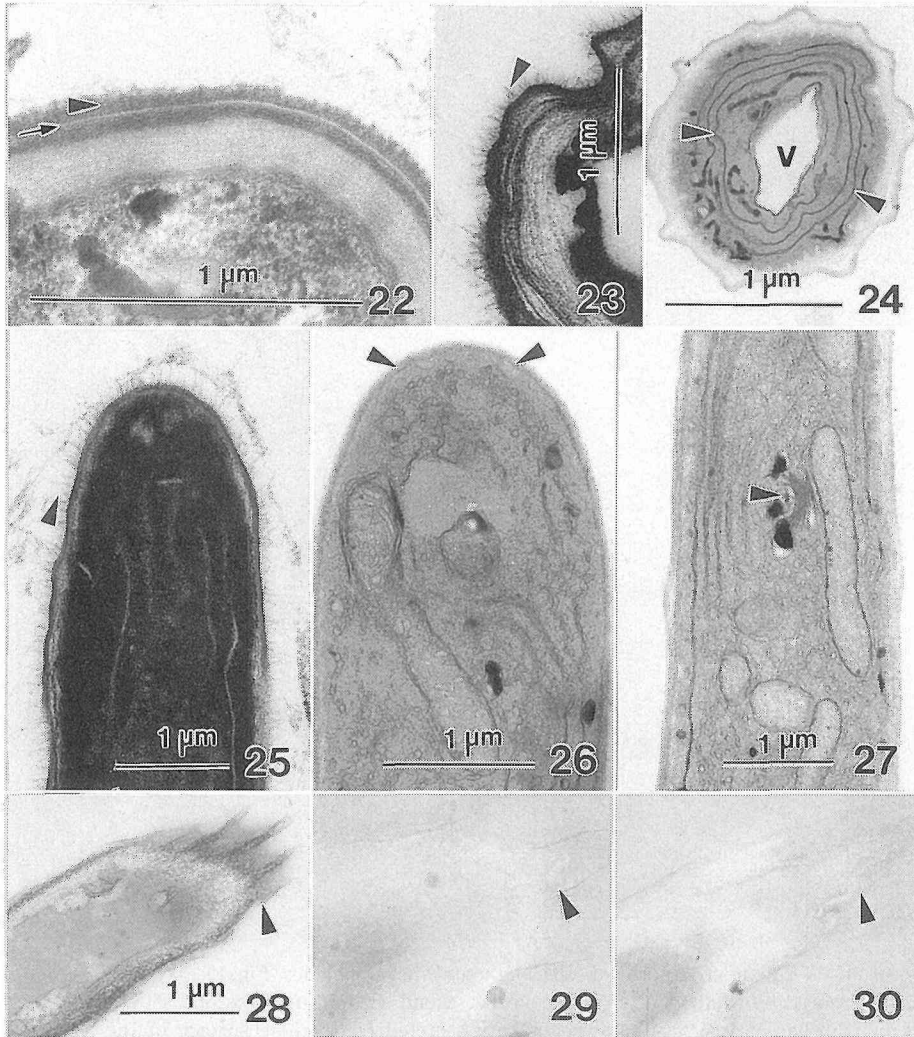
a gap formed between the spermatial plasma membrane and the spermatangial wall at a more advanced stage of spermatogenesis (Fig. 21).

Trichogyne and carpogonium

Trichogynes, in contrast to spermata, appeared to have no or very thin transparent covering on their cell walls under the light microscope (Fig. 33). However, the TEM specimens fixed by Method C and D showed that the cell wall surface of the trichogyne was uniformly coated with a fibrous trichogyne coat (Figs. 22, 23). The thicknesses of the coat in the specimens prepared by Methods C and D were about 20-30 nm and 80-100 nm, respectively. In longitudinal section, the trichogyne coat uniformly appeared even on the cell wall at the trichogyne apex (Fig. 25). In addition, the cell wall thickness in cross section was almost even in the Method C specimens (Fig. 22), whereas it was un-



Figs. 19-21. TEM micrographs of spermatangial development. Fig. 19. Young spermatangium. Prepared by Method A. Fig. 19a is the second section after the one shown in Fig. 19b. Electron-transparent vesicles (arrowheads) are secreted from whole surface of the spermatial cell inside the spermatangial cell wall. Fig. 20. Young spermatangium. Method D. The secreted vesicles (arrowheads) contain fibrous, reticulate material. Fig. 21. Spermatangium at a more advanced stage. Method D. Fibrous, reticulate material is observed in the gap (arrowheads) formed between the spermatial cell and spermatangial cell wall. Scale in Fig. 20 also applies to Fig. 21.



Figs. 22-30. TEM micrographs of trichogynes. Figs. 22-24. Cross section of median portion. Fig. 22. Prepared by Method C. Fibrous trichogyne coat (arrowhead) is observed uniformly on the surface of the trichogyne cell wall (arrow). Fig. 23. Method D. Radiating morphology of further enhanced trichogyne coat (arrowhead). Fig. 24. Method E. Note the concentric arrangement of endoplasmic reticulum (arrowheads) and a vacuole (V). Figs. 25, 26. Longitudinal section of trichogyne apex. Fig. 25. Method D. Fibrous trichogyne coat (arrow) is observed uniformly on the surface of the trichogyne apex. Fig. 26. Method E. Small vesicles (arrowheads) are secreted to the apical thin cell wall, and well-developed endoplasmic reticula

even in the specimens fixed by Method D and E (Figs. 23, 24).

The trichogyne coat was composed of a PATAg-positive material (Figs. 28, 29). The positive reaction of the PATAg test mostly disappeared after periodic acid oxidation followed by sodium borohydride reduction (Fig. 30). The periodic acid-sodium borohydride treatment thus appeared to destroy the PATAg-positive component, i. e., vicinal glycol residues, of the trichogyne coat.

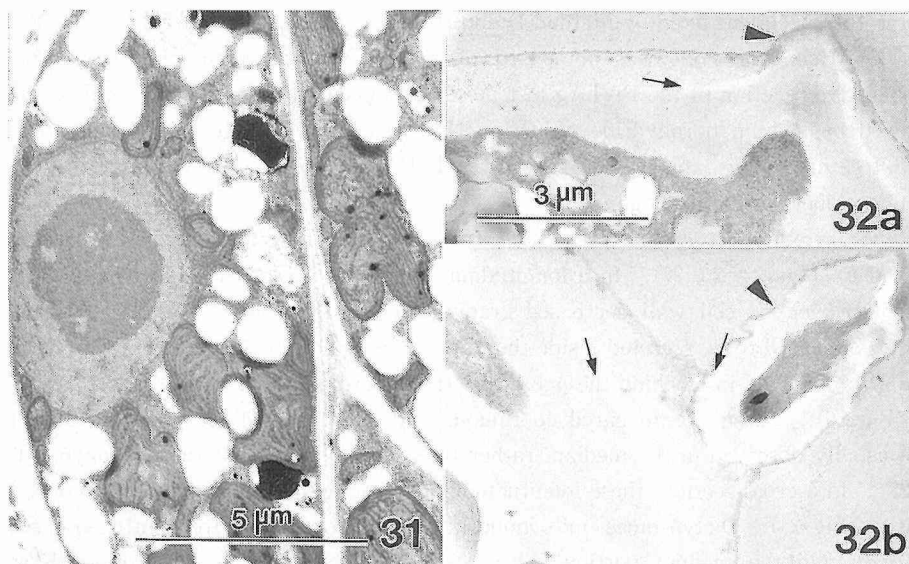
The membranous structures of the trichogyne cytoplasm were made visible by Method E (Figs. 24, 26, 27). In a longitudinal section of Method E specimens, the thickness of trichogyne cell wall decreased gradually toward the apex (Figs. 26, 27). Small vesicles appeared to be secreted inside the thin apical cell wall (Fig. 26). Similar vesicles were also observed just behind the apex, and these were associated with densely arranged ER (Fig. 26). These ER appeared continuous with the longitudinally arranged ER that were usually observed in the median, rather than apical, portion of the trichogyne (Figs. 26, 27). In a cross section, these longitudinal ER appeared to be arranged in a concentric manner (Fig. 24). Dictyosomes, mitochondria and vacuoles were frequently observed at the apex and the median portion (Figs. 24, 26, 27). No plastids or proplastids were found in the trichogyne cytoplasm (Figs. 24, 26, 27).

The carpogonial base was distinctly pigmented and swollen in contrast to the trichogyne and, like other vegetative cells of female gametophytes, contained numerous plastids and starch grains (Fig. 31). The carpogonial nucleus had dispersed chromatin and a distinct nucleolus. In TEM specimens prepared by Method A and B, cell walls of female germlings did not have an obvious fibrous appearance and two layers could be distinguished in the wall of the female thalli: an inner cell wall and an outer cell wall (Fig. 32). Both types of wall appeared to contain similar amorphous structures.

Stainability was slightly stronger in the inner wall than in the outer wall. The inner wall was outlined by a thin, electron-transparent layer (Fig. 32). The outer wall was well-developed along the surface of the thalli but was not detected between the cells. The trichogyne cell wall was continuous with the inner cell wall (Fig. 32); that is, though it is coated, the trichogyne is the particular site where the inner wall of female thalli is exerted and exposed to the external environment.



are visible adjacent to the vesicles. Fig. 27. Longitudinal section of median portion of trichogyne. Method E. Mitochondria and a dictyosome (arrowhead) are visible. Figs. 28-30. Oblique sections of trichogynes after PATAg test. Scale in Fig. 28 also applies to Figs. 29, 30. Figs. 28, 29. Untreated trichogynes. Fig. 28. Periodic acid oxidation in PATAg test. Trichogyne coat (arrowhead) shows positive reaction. Fig. 29. Hydrogen peroxide control of PATAg test. Trichogyne coat (arrowhead) is negatively stained. Fig. 30. Trichogyne after oxidation by periodic acid-sodium borohydride treatment. Periodic acid oxidation in PATAg test. Trichogyne coat (arrowhead) is very weakly stained.



Figs. 31, 32. TEM micrographs of female gametophyte. Fig. 31. Carpogonial base showing median section of carpogonial nucleus. Method B. Fig. 32. Oblique section of the basal portion of trichogyne (arrowheads). Method A. Arrows indicate the electron-transparent outline of the inner cell wall of a female gametophyte. Fig. 32b is the second section after the one shown in Fig. 32a.

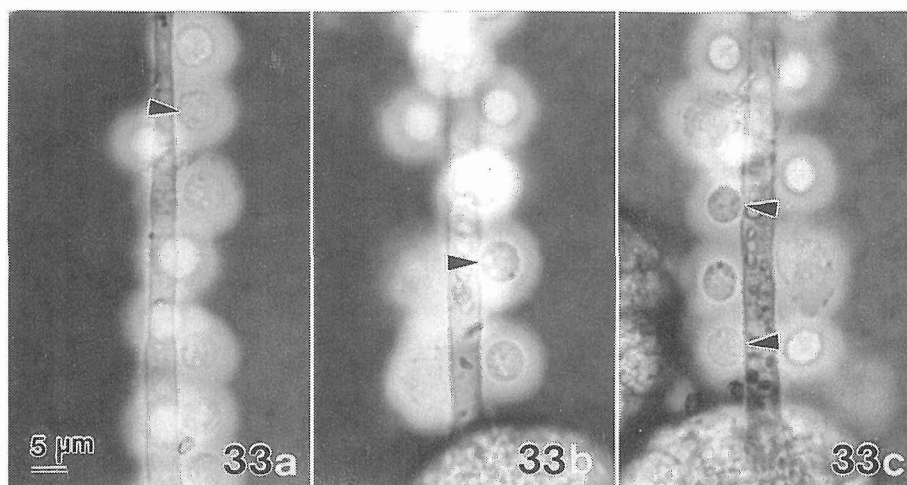
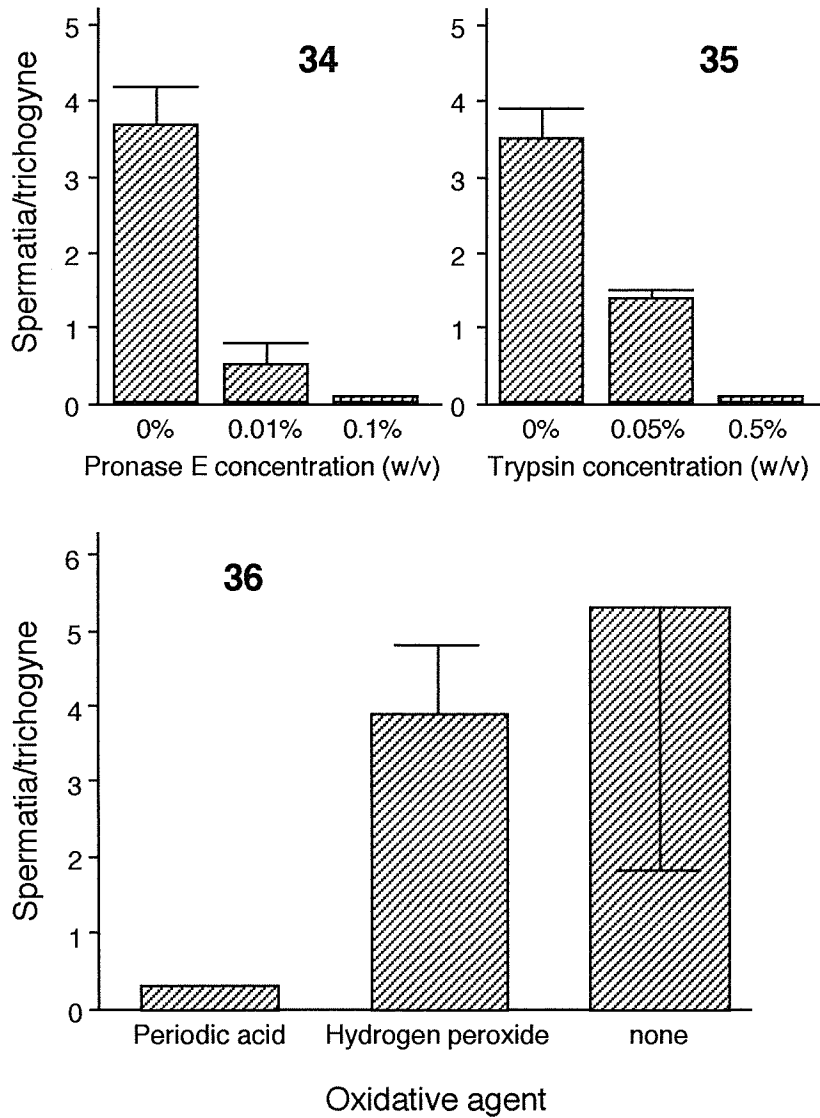


Fig. 33. Three examples of light micrographs of attachment of spermata to the trichogyne. Non-fixed material 5 min after spermatium inoculation. Prepared in India ink/seawater. Elimination of spermatial covering has occurred only at the site of attachment (arrowheads).



Figs. 34-36. Effect of pretreatment of gametes on gamete attachment. Degree of gamete attachment was expressed by the number of attached spermatia per trichogyne. Data were redrawn from MINE and TATEWAKI 1994b. Figs. 34, 35. Pretreatment of spermatia. Fig. 34. Effect of Pronase E preincubation. Fig. 35. Effect of trypsin preincubation. Fig. 36. Effect of degradation of vicinal glycols of the trichogyne coat.

Gamete attachment

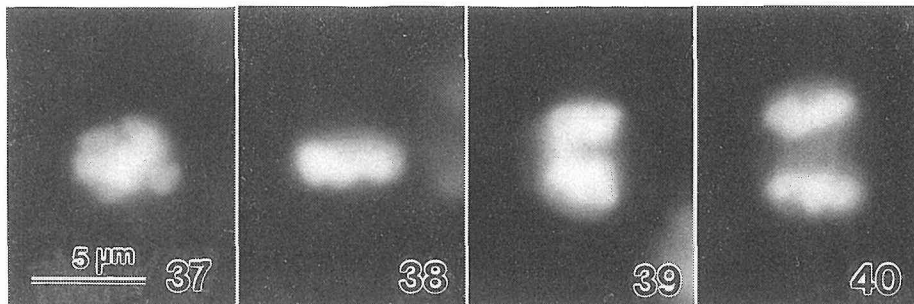
Within five minutes after spermatium inoculation, direct attachment of the spermatial plasma membrane to the trichogyne coat was observed in light microscope (Fig. 33) and TEM specimens (MINE and TATEWAKI 1994a). The covering of these spermatia appeared to have a uniform thickness, as observed in the liberated spermatia, except for the portion where the spermatium was attached to the trichogyne, indicating that localized elimination of the spermatial coverings rapidly occurred upon attachment of the gametes.

The gamete surfaces were disorganized in various ways to see how this might affect attachment of the spermatia to the trichogynes. Brief pretreatment (5 min) of spermatia with proteases inhibited their attachment to the trichogyne, and inhibition became conspicuous with increasing protease concentration (Figs. 34, 35). On the other hand, degradation of the trichogyne coat by periodic acid oxidation and sodium borohydride reduction also inhibited gamete attachment significantly (Fig. 36).

Spermatial nuclear division

After the attachment of spermatia to trichogynes, the division of the prophase nucleus of the spermatium proceeded to completion by 60 min. In the DAPI-stained specimens fixed 15 to 60 min after spermatium inoculation, further condensation of chromosomes (Fig. 37), alignment of the chromosomes along a metaphase plate (Fig. 38), the chromosomes segregation toward the opposite poles (Fig. 39) and binucleate spermatia (Fig. 40) were observed.

In the TEM specimens fixed by Method B, the ultrastructure of spermatial nuclei at various mitotic stages was observed. Prometaphase nuclei with further condensed chro-

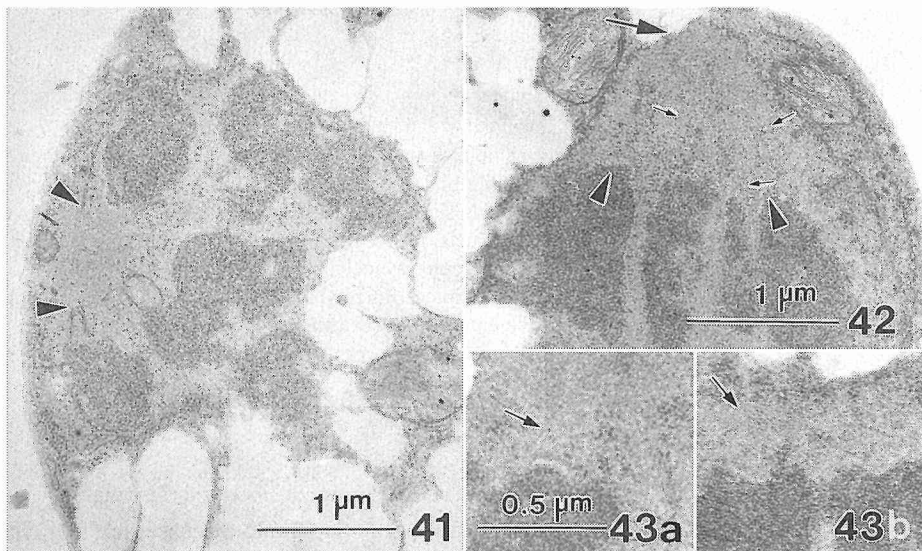


Figs. 37-40. Epifluorescence micrographs of spermatial nuclear division. DAPI-stained. Scale in Fig. 37 also applies to Figs. 38, 39, 40. Fig. 37. Further condensation of chromatin, or chromosomes, in prometaphase nucleus observed 15 min after spermatium inoculation. Fig. 38. Chromosomes aligned at the metaphase plate at 30 min. Fig. 39. An anaphase nucleus showing chromosome segregation at 45 min. Fig. 40. Spermatium after completion of nuclear division at 60 min.

mosomes in a disordered arrangement were frequently observed in the specimens fixed 15 min after spermatium inoculation (Fig. 41). At the polar region of these nuclei, a single nuclear envelope gap was formed and PRs could no longer be detected.

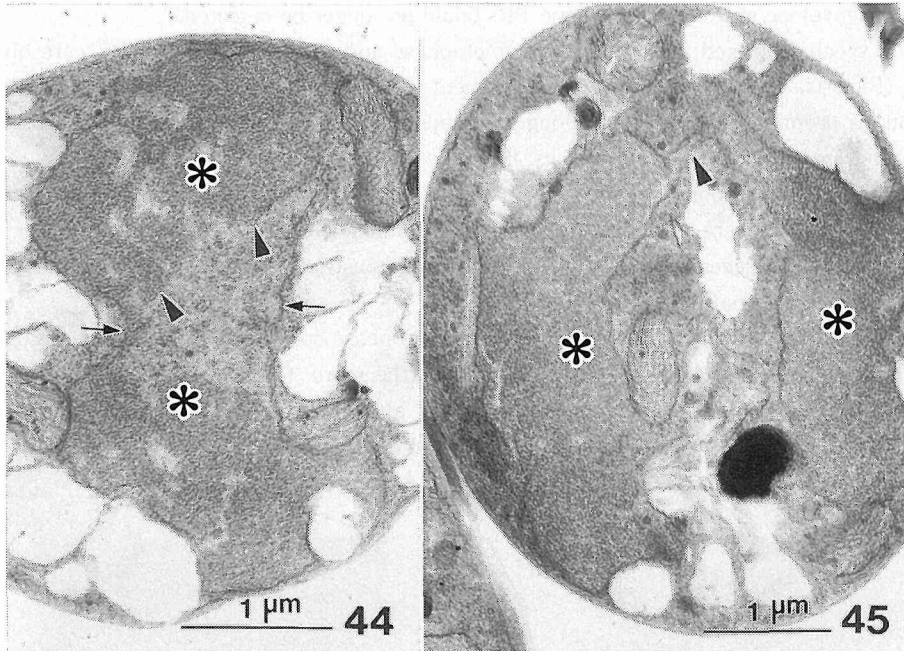
In specimens fixed at 30 min, many metaphase and early anaphase nuclei were observed (Figs. 42, 43). In these nuclei, alignment of chromosomes and their segregation toward a prominent polar region along the inside of the nucleus were seen. Chromosomes appeared to bear kinetochores (Figs. 42, 43) which were associated with several MTs directed toward the polar regions. In telophase nuclei observed in 45-min specimens, two derivative nuclei were reformed either by detachment from the interzonal midpiece and nuclear envelope regeneration (Fig. 44), or by the constriction of the nuclear envelope in the median interzonal midpiece (Fig. 45).

The plasma membranes of all of these post-prophase spermatia were attached directly to the cell wall surface of the trichogyne. Furthermore, the plasma membrane of the spermatia that remained uninucleate 180 min after spermatium inoculation was not attached directly to the trichogynes (MINE and TATEWAKI 1994a), indicating that the



Figs. 41-43. TEM micrographs of spermatial nuclear division. Prepared by Method B. Fig. 41. A nucleus in prometaphase condition 15 min after spermatium inoculation. Arrowheads indicate the edge of a nuclear envelope gap around the polar region. Fig. 42. Early anaphase nucleus at 30 min. Fully condensed chromosomes with kinetochores (arrowheads) have moved slightly toward the polar region (large arrow) from the metaphase plate. Small arrows indicate microtubules. Fig. 43. Examples of kinetochores observed in other metaphase or anaphase nuclei. Microtubules that appear to be associated with the kinetochore are indicated by arrows.

spermatial nuclear division resumed after the direct attachment of gametes.



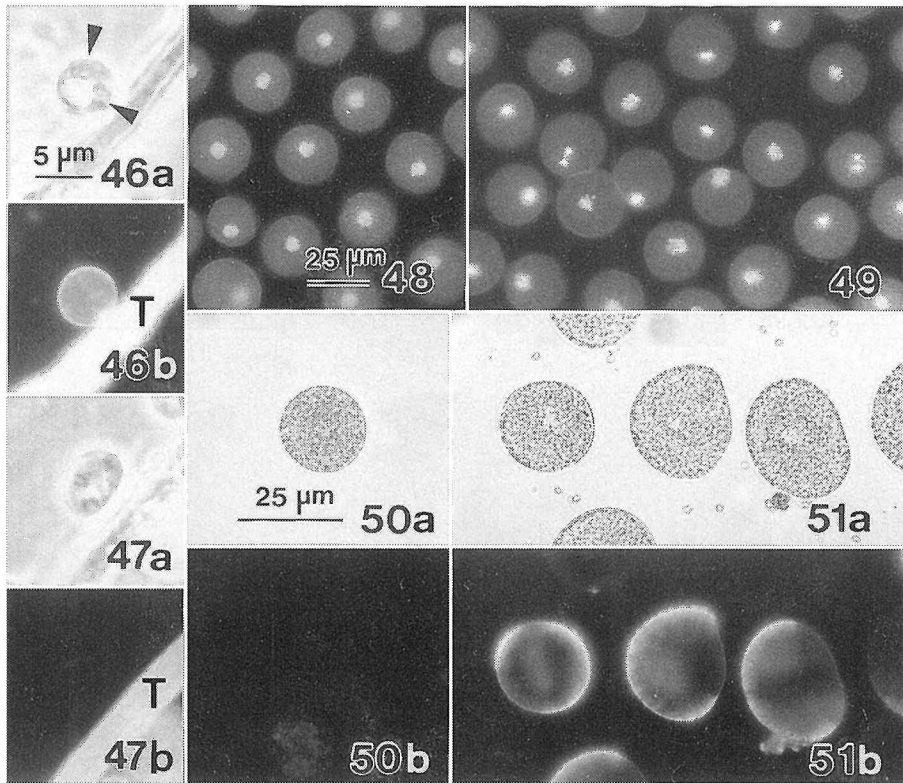
Figs. 44, 45. TEM micrographs of early telophase nuclei of spermatium. Forty-five minutes after spermatium inoculation. Prepared by Method B. Asterisks indicate segregated derivative nuclei. Fig. 44. An early telophase nucleus showing partial regeneration of nuclear envelopes (arrowheads) along derivative nuclei. Nuclear envelopes around interzonal midpiece are indicated by arrows. Fig. 45. Another early telophase nucleus. The derivative nuclei are separated by the constriction of the interzonal midpiece (arrowhead). Cytoplasmic components such as large vesicles and mitochondria have entered between the derivative nuclei.

Cell wall formation

Calcofluor-positive materials were not detected around liberated spermatia. However, they could be seen on attached, binucleate spermatia 60 min after spermatium inoculation (Fig. 46) while they were not detectable around the spermatia that remained uninucleate (Fig. 47). In addition, freshly liberated tetraspores of *Palmaria* sp. were not covered with calcofluor-positive materials (Figs. 50), and they secreted cell wall materials (Fig. 51) during the initial stages of germination (Figs. 48, 49).

Gamete fusion

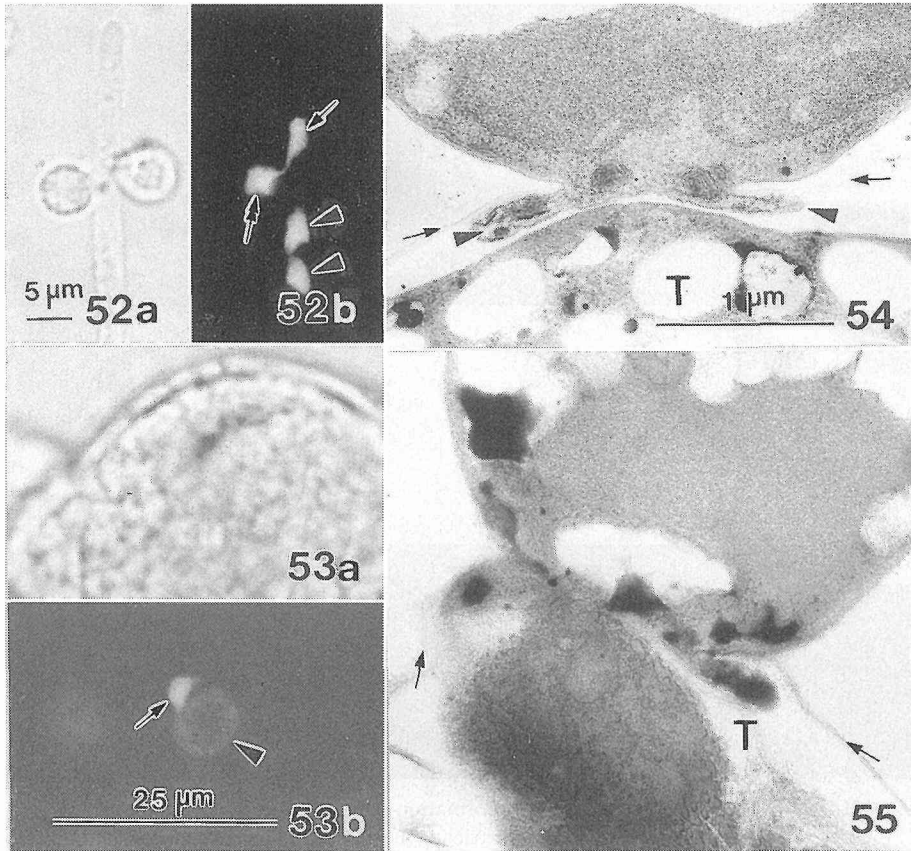
Cytoplasmic fusion of the binucleate spermatium with the trichogyne was followed by



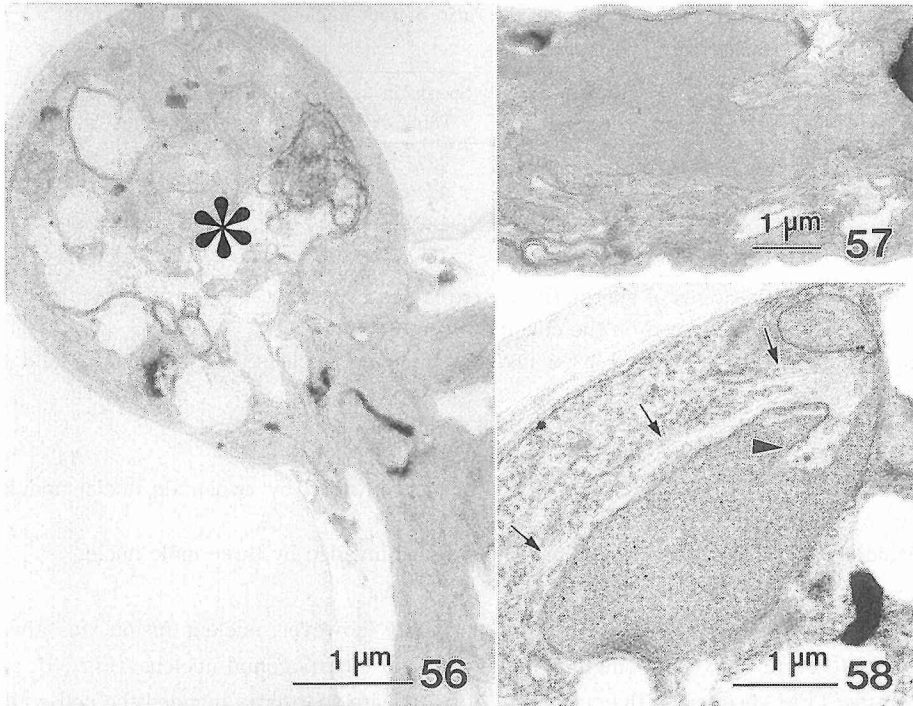
Figs. 46-51. Light micrographs of cell wall formation of spermatia and germinating tetraspores. Figs. 46, 47. Spermatium attached to a trichogyne (T). Non-fixed material 60 min after spermatium inoculation. Stained with calcofluor. a) Phase contrast. b) Epifluorescence. Scale in Fig. 46 also applies to Fig. 47. Fig. 46. Spermatium containing two derivative nuclei (arrowheads). Calcofluor-positive material is seen around the spermatium. Fig. 47. Uninucleate spermatium. Spermatial surface is not stained with calcofluor. Figs. 48-51. Cell wall formation of tetraspores of *Palmaria* sp. during germination. Figs. 48, 49. Epifluorescence micrographs of DAPI-stained specimens. Scale in Fig. 48 also applies to Fig. 49. Fig. 48. Sixty minutes after spore inoculation. Fig. 49. Eighteen hours. Metaphase or anaphase nuclei are visible. Figs. 50, 51. Calcofluor-stained. a) Bright field. b) Epifluorescence. Scale in Fig. 50 also applies to Fig. 51. Fig. 50. Liberated tetraspore. No fluorescence is detected. Fig. 51. Sixty minutes after inoculation. Calcofluor-positive material is detected around the cell surface.

the entrance of the derivative nuclei (male nuclei) into the trichogyne cytoplasm (Fig. 52). Male nuclei then migrated toward either the apex or the base of the trichogyne. The direction of the migration seemed to be at random.

The time course of changes in the nuclear behavior of the attached spermatia was examined in fertilization experiments conducted five times. The spermatial nuclear



Figs. 52-55. Gamete fusion. Figs. 52-53. Light micrographs. DAPI-stained. a) Bright field. b) Epifluorescence. Fig. 52. Invasion and migration of male nuclei to the trichogyne 60 min after spermatium inoculation. One derivative nucleus (arrow) of the spermatium has invaded and migrated toward the apex of the trichogyne whereas another (double arrow) remains in the cell. Arrowheads indicate male nuclei from another fused spermatium migrating toward the base of the trichogyne. Fig. 53. Nuclear fusion of a carpogonial nucleus (arrowhead) with a condensed male nucleus (arrow) at 180 min. Carpogonial nucleus contains unstained nucleolus. Figs. 54, 55. TEM micrographs of cytoplasmic fusion of a binucleate spermatium with trichogyne (T). Arrows indicate the trichogyne cell wall surface. Scale in Fig. 54 also applies to Fig. 55. Fig. 54. Spermatial cytoplasm (arrowheads) has invaded into the trichogyne cell wall and expanded. Sixty minutes after spermatium inoculation. Prepared by Method B. Fig. 55. Cytoplasmic fusion observed at 120 min. Method A.



Figs. 56-58. TEM micrographs of spermatial cell and male nuclei after cytoplasmic fusion observed 180 min after spermatium inoculation. Fig. 56. Opening between fused spermatial cell (asterisk) and trichogyne cytoplasm after invasion of two male nuclei. Prepared by Method A. Mitochondria and large vesicles have been left in the cytoplasm of the spermatium. Mitochondria and membranous structures are visible within the opening. Fig. 57. Male nucleus migrating in the trichogyne. Method A. Fig. 58. Male nucleus in carpogonial base associated with microtubules (arrows). Method B. An arrowhead indicates a microtubule-filled nuclear groove.

events were divided into four states that can be distinguished under a fluorescence microscope: state 1) undivided spermatial nucleus; state 2) spermatial nucleus divided into two male nuclei; state 3) one of the two male nuclei has entered into the trichogyne cytoplasm; and state 4) both male nuclei have entered into the trichogyne. The occurrence of these four states 30, 60, 120 and 180 min after spermatium inoculation is summarized in Table 1. As a result, more than half of the attached spermatia became binucleate by 60 min, though most of them were not divided at 30 min. At 180 min, about 30% of them had both of the derivative nuclei inserted into the trichogyne, whereas more than a third of the total spermatia remained uninucleate.

Thus, a number of male nuclei ordinarily invaded into a single trichogyne. Though the frequency was very low, the entrance of two or three male nuclei into the carpogonial

Table 1 Time course of changes in the ratio of four nuclear stages^a in all spermatia attached to the trichogyne.

Time (min)	Carpogonia			Spermatia				
	Total ^b	Invaded ^c	Karyogamy ^d	Total ^e	State1 (%)	State2 (%)	State3 (%)	State4 (%)
30	170	0	0	1272	98	2	0	0
60	211	0	0	1329	54	38	7	1
120	165	7	4 ^f	1379	43	22	18	17
180	184	18	40 ^g	1267	36	12	19	33

^a The four nuclear stages of spermatia are explained in results.

^b All the carpogonia formed on the coverslip were counted.

^c Carpogonia with carpogonial base invaded by male nucleus, but karyogamy did not occur.

^d Carpogonia where the carpogonial nucleus fused with male nucleus.

^e All the spermatia that attached to the trichogynes were counted.

^f Including two carpogonia with carpogonial base invaded by two male nuclei and karyogamy occurred with one of them.

^g Including one carpogonium with carpogonial base invaded by three male nuclei.

base was observed (Table 1). In the present study, however, nuclear fusion was always observed to occur between a single male nucleus and a carpogonial nucleus (Fig. 53).

In the TEM specimens, the cytoplasm of binucleate spermatia invaded the cell wall of the trichogyne and expanded within the cell wall before cytoplasmic fusion (Figs. 54, 55). Although the passage of the male nucleus through an opening between the trichogyne and fused spermatium was not observed, several organelles, e. g., mitochondria, large vesicles and unspecified membranous structures, were left in the spermatium and at the opening after the invasion of male nuclei (Fig. 56). However, because these structures were also present in trichogynes before fertilization, their origin remained unknown.

Migrating male nuclei in a trichogyne and carpogonial base were also observed by TEM (Figs. 57, 58). The invading male nucleus in the carpogonial base maintained a condensed appearance and was associated with a bundle of MTs (Fig. 58). Polar rings were not found around either the invading male nucleus or the co-existing carpogonial nucleus. Unfortunately, no occurrence of nuclear fusion was found in the TEM specimens.

Discussion

Spermatangial vesicles

The presence of large, mucilage-containing vesicles, or vacuoles, has been reported in the spermatogenesis of many species of red algae. The appearance of the contents, modes of formation and secretion of the vesicles vary according to species (see PUESCHEL 1990 for references). It was speculated that the function of these vesicles is to

supply a discharge force from the spermatangium (SCOTT and DIXON 1973) and to supply a secretion of mucilage strands, wall materials or sticky covering of liberated spermatium (PEEL and DUCKETT 1975, KUGRENS 1980, FETTER and NEUSHUL 1981).

In *Palmaria* sp., the large vesicles in spermatangia appeared to function in at least two ways during spermatogenesis and fertilization. The contents of vesicles secreted before spermatium liberation, judging from the present observations, may form the spermatial covering. Secretion of large vesicles within the spermatangium that contribute to the spermatial appendage formation have already been reported in several red algae (FETTER and NEUSHUL 1981, BROADWATER *et al.* 1991, KIM and FRITZ 1993b). The other vesicles of *Palmaria* sp. were never secreted out of the spermatium throughout fertilization, and occasionally served as a wedge between the derivative nuclei of spermatial nuclear division.

Spermatial nucleus

Nuclear division of spermatia generally occurs at a certain stage between spermatogenesis and fertilization in red algae. Binucleate spermatia have been reported (see GOFF and COLEMAN 1984 for references), and after liberation of spermatia, nuclear division occurs before gamete attachment in some species (e.g. *Choreocolax* [GOFF and COLEMAN 1984]). The TEM figures of liberated spermatia in *Corallina officinalis* showed that the spermatial nuclei were arrested at metaphase or anaphase of nuclear division (PEEL and DUCKETT 1975). Previous light microscopic studies, however, indicated that the mature spermatial nuclei of several red algae are in a prophase condition, as observed in the present study (GRUBB 1925, FRITSCH 1945, p. 596, DREW 1951, MAGNE 1952, MUMFORD and COLE 1977). Spermatial nuclear divisions were ordinarily found after attachment of uninucleate spermatia to trichogynes in *Nemalion* and *Batrachospermum* (see FRITSCH 1945, p. 597 for references).

The first ultrastructure of spermatial nuclear division to completion in red algae was demonstrated in *Palmaria* sp. (MINE and TATEWAKI 1994a). This report also presented a comparison of the ultrastructure of the spermatial nuclear division with those of somatic cell division in other red algae.

Nuclear envelopes have been observed to be intact in most TEM studies of red algal spermatia (e.g., PEEL and DUCKETT 1975, KUGRENS 1980, FETTER and NEUSHUL 1981, BROADWATER *et al.* 1991). The present study also showed intact nuclear envelopes during spermatogenesis and in the liberated spermatia. However, some earlier workers reported the absence of a nuclear envelope in mature spermatial nuclei (SCOTT and DIXON 1973, HAWKES 1978). Some methods that preserve the biological membranes, e.g., Method E in the present study, should be used in order to confirm the absence of the spermatial nuclear envelope reported in these studies.

In contrast to the condensed state of the spermatial or male nucleus throughout the

fertilization processes in *Choreocolax* (GOFF and COLEMAN 1984) or in *Palmaria* (MINE and TATEWAKI 1994a and the present study), HAWKES (1978) observed decondensation of the spermatial nucleus after attachment to the prototrichogyne in *Porphyra* and speculated that the decondensation occurs in order to "code for an enzyme required to make the fertilization canal". It would be of interest to determine whether the genes encoded in the male nucleus were expressed, and whether such expression is required during fertilization. Further examination of the morphology and physiology of the male nucleus will be necessary to resolve this problem.

In *Palmaria* sp., the strictly prophase-arrested nucleus of the liberated spermatium proceeded with nuclear division only after attachment of the spermatial plasma membrane to the trichogyne surface (MINE and TATEWAKI 1994a). This indicates the presence of a signal transduction mechanism that converts an extracellular stimulus (direct attachment of gametes) to an intracellular event (post-prophase progression of nuclear division). Fertilization of *Palmaria* sp. could be a potentially useful experimental system for studying the signal transduction mechanism of red algae and control of mitotic progression in lower eukaryotes. Recent investigations have revealed that the calcium influx and changes in the levels of a cellular cyclic nucleotide are involved in this mechanism (MINE and TATEWAKI 1994c, MINE 1996).

Carpogonium

Carpogonia have been studied previously using TEM in three species, *Porphyra gardneri* (HAWKES 1978), *Polysiphonia harveyi* (BROADWATER and SCOTT 1982) and *Nothocladus lindaueri* (SHEATH *et al.* 1996). The most noticeable differences in the cytoplasmic components of the carpogonia of these examples were the degree of plastid development and the presence (or absence) of starch grains. Fully developed plastids and numerous starch grains were observed in *Porphyra*, but only proplastids and no starch grains were detected in *Polysiphonia* and *Nothocladus*. Despite the similarities in external appearance (i. e., carpogonia with distinct trichogynes rather than undifferentiated prototrichogynes), the ultrastructure of the carpogonium of *Palmaria* sp. observed in the present study is quite different from that of *Polysiphonia* and *Nothocladus*.

On the other hand, prominent plastid development and numerous starch grains in the carpogonium or carpogonial base are features common to *Porphyra* and *Palmaria*. This is not surprising in consideration of recent arguments that, as is the order Bangiales, the order Palmariales is one of the most primitive groups of red algae (PUESCHEL and COLE 1982, GUIRY 1987).

As in *Polysiphonia* (BROADWATER and SCOTT 1982), the vesicle secretion at the trichogyne apex was also observed in *Palmaria* sp. Because the cell wall in *Palmaria* sp., unlike that in *Polysiphonia*, was very thin at the apex and its thickness gradually increased toward the median portion, it is possible that the vesicles secrete the cell wall

material rather than the coating material as speculated in *Polysiphonia* (BROADWATER and SCOTT 1982). In addition, the significant features in the trichogyne cytoplasm of *Palmaria* were the longitudinal, concentric arrangement of ER and the absence of both plastids and proplastids.

Gamete attachment

Two kinds of spermatial structures, the appendages and the covering, which potentially mediate gamete attachment in red algae, have been reported. Several types of spermatial appendages have been reported in the bangiacean and ceramiacean algae, including *Tiffaniella* (FETTER and NEUSHUL 1981; as spermatial strand), *Aglaothamnion* (MAGRUDER 1984), *Bangia* (COLE *et al.* 1985; as spermatial corn), *Spyridia* (BROADWATER *et al.* 1991), and *Antithamnion* (KIM and FRITZ 1993a, b).

Some of these studies showed that the spermatial appendages specifically attached to the surface of female gametes, indicating that they were responsible for the initial binding of gametes. In *Antithamnion*, this was confirmed by the fact that concanavalin A, a lectin that is bound to mannose, was specifically bound to the spermatial surface and appendages and that either preincubation of spermatia with concanavalin A or preincubation of trichogynes with mannose significantly inhibited gamete attachment (KIM and FRITZ 1993a).

On the contrary, a previous SEM study of *Halosaccion* (MITMAN and PHINNEY 1985) and the TEM studies of *Palmaria* (MINE and TATEWAKI 1994a, b and the present study) showed that spermatia of the palmariacean algae bore no appendage on the surface throughout the fertilization process, but that, in *Palmaria*, they were covered with semi-solid coverings of uniform thickness. Furthermore, the degradation of the covering by proteases remarkably inhibited gamete attachment.

A few studies have previously shown morphological differentiation in the receptive surface of red algal female gametes. An amorphous substance covered the trichogyne cell wall in *Polysiphonia*, which decreased in thickness from the tip to the base of the trichogyne (BROADWATER and SCOTT 1982). In *Bangia*, the spermatia attached to the wall coating where the intensity of outer wall staining for sulfated polysaccharides decreased (COLE *et al.* 1985). Recently, SHEATH *et al.* (1996) showed a thickened, electron-dense cell wall coat around the trichogyne apex in the batrachspermalean alga *Nothocladus lindaueri* to which the spermatia were preferentially attached upon fertilization.

In *Palmaria*, the vicinal glycol residues of the fibrous trichogyne coat, which were detected as a PATAg-positive components, seemed to be essential for gamete attachment since the attachment was inhibited by specific chemical degradation. Although the PATAg-positive reaction can be interpreted in various ways, the majority of the positive compounds are 1-4 linked polysaccharides (ROLAND and VIAN 1991). As in the studies

of fertilization in other macroalgae (BOLWELL *et al.* 1979, KIM and FRITZ 1993a), investigations using sugars, lectins and specific glycosidases are necessary to understand the role of vicinal glycol residues of the adhesive trichogyne coat in gamete attachment.

As mentioned above, there are significant variations in the morphological and cytochemical characteristics of cell structures responsible for gamete attachment in red algae. In addition to this, the range of taxa in which interspecific gamete attachment and/or fusion occurred was quite different between the ceramiacean and palmariacean algae (MAGRUDER 1984, MINE and TATEWAKI 1993). To understand how such considerable variety of fertilization mechanisms has occurred in red algae, detailed, comparable information on the properties of gamete attachment apparatuses in different taxa is absolutely necessary.

Spermatial cell wall formation

In *Palmaria* sp., judging from their concomitant decrease and identity of their contents (MINE and TATEWAKI 1994a), the small, electron-dense vesicles probably contributed to the spermatial cell wall formation. Moreover, it is possible that the peripheral tubules, which were closely associated with both the plasma membrane and the small vesicles, were involved in the secretion of cell wall material.

There have been a few examples of cell structure being involved in the formation of cell coverings in red algae. Ultrastructural autoradiography of a unicellular red alga demonstrated that sulfation of extracellular mucilage was carried out in dictyosomes (EVANS *et al.* 1974). The resulting sulfated polysaccharides were probably secreted via vesicle secretion. A freeze fracture investigation of *Erythrocladia* and *Porphyra* showed putative microfibril-synthesizing complexes in the plasma membrane (TSEKOS and REISS 1992, 1994). The contribution of the vesicle and plasma membrane tubules to the spermatial cell wall formation in *Palmaria* spermatia has not been fully confirmed in the present study. However, the wide distribution of this structure in red algae (see PUESCHEL 1990, p. 10 for references) suggests that the plasma membrane tubule may potentially be one of the major structures involved in the formation of cell coverings in red algae.

The present study also confirmed that the liberated tetraspores of *Palmaria* sp. formed a calcofluor-positive structure on the cell surface after attachment to the substratum, and then commenced germination, i. e., cell division. Although the PATAg-positive vesicles have not been confirmed in tetraspores of *Palmaria*, there is an interesting similarity between the spermatial nuclear division and tetraspore germination. Both involve activation of cell wall formation and mitotic progression after attachment of the cell to an 'appropriate' substratum (i. e., the trichogyne coat for the spermatia and the substratum for tetraspore germination). Moreover, though the occurrence of small, electron-dense vesicles has not yet been confirmed, short-lived, "tubular plasmalemmal structures" were reported in tetraspores of *Palmaria palmata* (MANDURA *et al.* 1986). These peripheral

tubules, which are common structures in the reproductive cells of *Palmaria*, may possibly be involved in the recognition of cell-substratum contact and/or the secretion of the cell wall materials.

Gamete fusion

The ultrastructure of the gamete fusion process of red algae has been observed by HAWKES (1978) in *Porphyra gardneri*. In this instance, the "spermatial nuclear material" was transferred to the carpogonium via a narrow, extended fertilization canal. In *Porphyra*, the nuclear material appeared to be the first cytoplasmic component to be transferred into the fertilization canal, and that other components, such as proplastids, followed the nuclear material into the canal (HAWKES 1978). In contrast, the cytoplasm of the attached spermatium of *Palmaria* sp. formed an expanded opening within the trichogyne cell wall before cytoplasmic fusion. The resulting large opening between the spermatium and trichogyne cytoplasm apparently assured transfer of the invading male nucleus with minimum constriction.

The present study is the first ultrastructural report of the male (spermatial) nucleus invading the carpogonium of red algae. The most striking feature of the male nucleus invading the carpogonial base of *Palmaria* sp. was the association of MTs. During fertilization of fucoid brown algae, nuclear migration of the male pronucleus toward the co-existing egg nucleus was inhibited by MT inhibitors (BRAWLEY and QUATRANO 1979, SWOPE and KROPPF 1993), implying that MTs played an indispensable role in the joining of the nuclei in fertilization of this alga. The remarkable MT association with the male nucleus in the carpogonial base of *Palmaria* sp. was similarly suggestive of the function of MTs in the migration of the male nucleus to the carpogonial nucleus.

Summary

Structures and processes in fertilization of the red alga *Palmaria* sp. were observed using light, epifluorescence and transmission electron microscopes. Precise time-course examination was possible using this alga, because it formed rapidly-maturing microscopic female gametophytes and macroscopic male gametophytes liberating spermatia vigorously.

The liberated spermatium had a single prophase nucleus and was covered with a colorless, semi-solid covering of uniform thickness. The spermatial covering was apparently produced during spermatogenesis before liberation of the spermatium. The spermatial covering was degraded by certain proteases.

In the cytoplasm of the trichogyne, dictyosomes, mitochondria and concentric, longitudinally-arranged endoplasmic reticulum (ER) were observed. Secretion of small vesicles apparently derived from the ER was detected in the apex of trichogyne. The cell wall of the trichogyne was covered with a fibrous coat.

Immediately after spermatium inoculation, the attachment of the spermatial covering

to the trichogyne coat was established. Within 5 min after inoculation, the spermatial covering was eliminated completely only at the site of attachment, resulting in the direct attachment of the spermatial plasma membrane to the trichogyne cell wall surface.

The gamete attachment was effectively inhibited by brief pretreatment of spermatia with proteases as well as by chemical destruction of vicinal glycol residues of the trichogyne coat.

After the direct attachment of gametes, the prophase-arrested spermatial nucleus resumed nuclear division. The completion of spermatial nuclear division (telophase) was observed 45 min after spermatium inoculation. Examination of TEM specimens indicated that direct attachment of gametes was necessary for the resumption of spermatial nuclear division. As the spermatial nuclear division proceeded, cell wall material, recognized as calcofluor-positive material, formed around the spermatium.

The cytoplasm of the binucleate spermatium invaded and expanded within the trichogyne cell wall before the cytoplasmic fusion of gametes. Both of the two derivative (male) nuclei of the spermatial nuclear division entered the trichogyne cytoplasm and migrated toward either the apex or the base of the trichogyne. The trichogyne could fuse with multiple spermatia and many male nuclei were observed to enter the trichogyne cytoplasm. However, as far as was observed in the present study, the number of male nuclei that invaded into a carpogonial base was no more than three and a carpogonial nucleus always fused with a single male nucleus.

The male nucleus that invaded the carpogonial base was associated with a number of microtubules. The male nucleus maintained its condensed state until nuclear fusion with a carpogonial nucleus.

Literature Cited

- BOLWELL, G. P., CALLOW, J. A., CALLOW, M. E. and EVANS, L. V.
1979. Fertilization in brown algae. II. Evidence for lectin-sensitive complementary receptors involved in gamete recognition in *Fucus serratus*. J. Cell Sci. **36**: 19-30.
- BRAWLEY, S. H. and QUATRANO, R. S.
1979. Effects of microtubule inhibitors on pronuclear migration and embryogenesis in *Fucus distichus* (Phaeophyta). J. Phycol. **15**: 266-272.
- BROADWATER, S. T. and SCOTT, J.
1982. Ultrastructure of early development in the female reproductive system of *Polysiphonia harveyi* BAILEY (Ceramiaceae, Rhodophyta). J. Phycol. **18**: 427-441.
- BROADWATER, S. T., SCOTT, J. L. and WEST, J. A.
1991. Spermatial appendages of *Spyridia filamentosa* (Ceramiaceae, Rhodophyta). Phycologia **30**: 189-195.
- COLE, K. M., PARK, C. M., REID, P. E. and SHEATH, R. G.
1985. Comparative studies on the cell walls of sexual and asexual *Bangia atropurpur-*

- ea* (Rhodophyta). I. Histochemistry of polysaccharides. *J. Phycol.* **21**: 585-592.
- DESHMUKHE, G. V. and TATEWAKI, M.
1990. The life history and evidence of the macroscopic male gametophyte in *Palmaria palmata* (Rhodophyta) from Muroran, Hokkaido, Japan. *Jpn. J. Phycol.* **38**: 215-222.
- DIXON, P. S.
1973. *Biology of the Rhodophyta*. Hafner, New York.
- DREW K. M.
1951. Rhodophyta. In G. M. SMITH (ed.), *Manual of Phycology*. Chronica Botanica Co., Waltham, Mass. pp.167-191.
- EVANS, L. V., CALLOW, M. E., PERCIVAL, E. and FAREED, V.
1974. Studies on the synthesis and composition of extracellular mucilage in the unicellular red alga *Rhodella*. *J. Cell Sci.* **16**: 1-21.
- FETTER, R. and NEUSHUL, M.
1981. Studies on developing and released spermatia in the red alga, *Tiffaniella snyderae* (Rhodophyta). *J. Phycol.* **17**: 141-159.
- FRITSCH, F. E.
1945. *The structure and reproduction of algae*. vol. II. 939 pp.+xii. Cambridge University Press, Cambridge.
- GOFF, L. J. and COLEMAN, A. W.
1984. Elucidation of fertilization and development in a red alga by quantitative DNA microspectrofluorometry. *Dev. Biol.* **102**: 173-194.
- GRUBB, V. M.
1925. The male organs of the Florideae. *J. Linn. Soc. (Bot.)* **47**: 177-255.
- GUIRY, M. D.
1987. The evolution of life history types in the Rhodophyta: an appraisal. *Cryptogam. Algol.* **8**: 1-12.
- HAWKES, M. W.
1978. Sexual reproduction in *Porphyra gardneri* (SMITH *et* HOLLENBERG) HAWKES (Bangiales, Rhodophyta). *Phycologia* **17**: 329-353.
- HOMMERSAND, M. H. and FREDERICQ, S.
1990. Sexual reproduction and cystocarp development. In K. M. COLE and R. G. SHEATH (eds.), *Biology of the red algae*. Cambridge University Press. pp.305-345.
- KIM, G. H. and FRITZ, L.
1993a. Gamete recognition during fertilization in a red alga *Antithamnion nipponicum*. *Protoplasma* **174**: 69-73.
1993b. Ultrastructure and cytochemistry of early spermatangial development in *Antithamnion nipponicum* (Ceramiaceae, Rhodophyta). *J. Phycol.* **29**: 797-805.
- KUGRENS, P.

1980. Electron microscopic observations on the differentiation and release of spermatia in the marine red alga *Polysiphonia hendryi* (Ceramiales, Rhodomelaceae). *Amer. J. Bot.* **67**: 519-528.
- MAGNE, F.
1952. La structure du noyau et le cycle nucléaire chez le *Porphyra linearis* GREVILLE. *C. R. Acad. Sci. Paris* **234**: 986-988.
- MAGRUDER, W. H.
1984. Specialized appendages on spermatia from the red alga *Aglaothamnion neglectum* (Ceramiales, Ceramiaceae) specifically bind with trichogynes. *J. Phycol.* **20**: 436-440.
- MANDURA, A., BONEY, A. D. and BOWES, B. G.
1986. Tubular plasmalemmal structures in newly released spores of some red algae. *Nova Hedwigia* **42**: 277-282.
- MINE, I. and TATEWAKI, M.
1993. Life history of *Halosaccion yendoi* I. K. LEE (Palmariales, Rhodophyta) and interspecific spermatium inoculation with *Palmaria* sp. from Hokkaido, Japan. *Jpn. J. Phycol.* **41**: 123-130.
1994a. Attachment and fusion of gametes during fertilization of *Palmaria* sp. (Rhodophyta). *J. Phycol.* **30**: 55-66.
1994b. Gamete surfaces and attachment during fertilization of *Palmaria* sp. (Palmariales, Rhodophyta). *Jpn. J. Phycol.* **42**: 291-299.
1994c. Progression of spermatial nuclear division requires calcium influx during fertilization of the red alga *Palmaria* sp. *J. Phycol.* **30**: 853-856.
- MINE, I.
1996. Progression of spermatial nuclear division during fertilization of the red alga *Palmaria* sp. *Mem. Fac. Sci. Kochi Univ. Ser. D (Biol.)* **16/17**: 29-33.
- MITMAN, G. G. and PHINNEY, H. K.
1985. The development and reproductive morphology of *Halosaccion americanum* I. K. LEE (Rhodophyta, Palmariales). *J. Phycol.* **21**: 578-584.
- MUMFORD, Jr., T. F. and COLE, K.
1977. Chromosome numbers for fifteen species in the genus *Porphyra* (Bangiales, Rhodophyta) from the west coast of North America. *Phycologia* **16**: 373-377.
- PEEL, M. C. and DUCKETT, J. G.
1975. Studies of spermatogenesis in the Rhodophyta. *Biol. J. Linn. Soc.* **7** (suppl. 1): 1-13.
- PUESCHEL, C. M.
1990. Cell structure. *In* K. M. COLE and R. G. SHEATH (eds.), *Biology of the red algae*. Cambridge University Press. pp. 7-41.
- PUESCHEL, C. M. and COLE, K. M.

1982. Rhodophycean pit plugs: an ultrastructural survey with taxonomic implications. *Am. J. Bot.* **69**: 703-720.
- ROLAND, J. C. and VIAN, B.
1991. General preparation and staining of thin sections. In J. L. HALL and C. HAWES (eds.), *Electron microscopy of plant cells*. Academic Press, London. pp. 1-66.
- SCOTT, J. and BROADWATER, S.
1990. Cell division. In K. M. COLE and R. G. SHEATH (eds.), *Biology of the red algae*. Cambridge University Press, Cambridge. pp. 123-145.
- SCOTT, J. L. and DIXON, P. S.
1973. Ultrastructure of spermatium liberation in the marine red alga *Ptilota densa*. *J. Phycol.* **9**: 85-91.
- SHEATH, R. G., MÜLLER, K. M., WHITTICK, A. and ENTWISLE, T. J.
1996. A re-examination of the morphology and reproduction of *Nothocladus lindaueri* (Batrachospermales, Rhodophyta). *Phycol. Res.* **44**: 1-10.
- SWOPE, R. E. and KROPF, D. L.
1993. Pronuclear positioning and migration during fertilization in *Pelvetia*. *Dev. Biol.* **157**: 269-276.
- TSEKOS, I. and REISS, H. D.
1992. Occurrence of the putative microfibril-synthesizing complexes (linear terminal complexes) in the plasma membrane of the epiphytic marine red alga *Erythrocladia subintegra* ROSENV. *Protoplasma* **169**: 57-67.
1994. Tip cell growth and the frequency and distribution of cellulose microfibril-synthesizing complexes in the plasma membrane of apical shoot cells of the red alga *Porphyra yezoensis*. *J. Phycol.* **30**: 300-310.
- VAN DER MEER, J. P.
1981. The life history of *Halosaccion ramentaceum*. *Can. J. Bot.* **59**: 433-436.
- VAN DER MEER, J. P. and TODD, E. R.
1980. The life history of *Palmaria palmata* in culture. A new type for the Rhodophyta. *Can. J. Bot.* **58**: 1250-1256.